Short backfire antenna aperture distribution control by cavity profile shaping

Derek GRAY and L. SHAFAI
TRLabs *also with* Dept. of ECE, University of Manitoba
Winnipeg, Manitoba, Canada R3T 5V6
E-mail dgray@ee.umanitoba.ca

1. Introduction

A number of high aperture efficiency waveguide fed horn arrays, which have a height of several wavelengths (λ_o), have recently been investigated at millimetre wave frequencies for civilian applications [1]. Two low profile alternatives to horn antennas are cavity antennas overlain with a slotted screen ($\approx 0.875\lambda_o$) [2] and short backfire antennas ($\approx 0.5\lambda_o$) [3]. A large scale, dual polarised, waveguide fed array of short backfire antennas (SBA) has been proposed for DBS television reception (about 12GHz) [4]. Such structurally robust and readily die cast arrays are also of interest for upperband linearly polarised MMDS, LMCS and LMDS subscriber antennas (25.35-31.3GHz), and can be potentially manufactured at low cost. However, waveguide fed SBAs are not well understood and have only been studied for a few distinct cavity diameters and depths. There is, thus, a need for a wideranging parametric study of SBAs before arraying can be considered, and a modern numerical tool such as Ansoft HFSS™ ver. 6.0 would be applicable. The aim is to design a large array element, allowing sufficient lateral space to accommodate the waveguide feeding network (and matching stubs if element input impedance requires matching), with high directivity and nulls placed for grating lobe suppression. Two different circularly symmetric cavity profiles fed by rectangular waveguide were investigated across a range of diameters, and the aperture amplitude and phase distributions of the two types compared. The more readily die cast design was found to give higher directivity and characteristics more amenable to arraying from a larger diameter antenna.

2. Model

All trials were conducted using the commercially available finite element method software HFSS. All cavities investigated had a depth of $0.5\lambda_o$. Subreflectors were planar, infinitely thin, had a diameter of $0.5\lambda_o$, and set in the centre of the cavity mouth, Figure 1. The subreflectors would be suspended from a thin dielectric film in experimental units. Inset waveguide feeds, if used, were inset $0.25\lambda_o$. A radiation space was required for radiating structures modeled in HFSS; a prism of $3.3\text{x}3.3\text{x}0.5\lambda_o$ (66x66x10mm) filled with vacuum was used for this purpose, which meant that all cavities were set into an infinite conducting sheet presumably approximating behaviour within a large array environment. For all trials, the boundaries of the radiation space were seeded with triangles of side no greater than $0.1\lambda_o$ (2mm) so that the radiation boundaries of all models would be comparable, irrespective of how many iterations were taken by the solver to reach the solution criteria of max. $\delta S=0.02$. The design frequency was 15GHz, having a free space wavelength (λ_o) of 20mm, and WR-62 rectangular waveguide was used. This would ease the requirements of manufacturing tolerances in prototype experimental units, and all dimensions would later be halved for operation about 30GHz.

3. Different Profiles

Two different cavity profiles have been investigated. The first design (A) was the typical flat based, inset fed cylindrical cavity [2]. The second design (B) likewise had a flat base, but the juncture of the cavity base and rim was curved with a radius of 10mm.

4. Discussion

Good agreement has been found to the cross-polar level (-30dB) between experimental and HFSS results for a inset fed, $2.5\lambda_o$ diameter, flat based, type (A) SBA for the prediction of null and sidelobe angular positions, although the directivity was lower than that measured experimentally, Figure 2. The well defined nulls at 23° (position of the grating lobes for an array of $2.5\lambda_o$ elements) in the experimental H-plane radiation pattern appear as a shoulder in both HFSS models with identical dimensions to the experimental antenna and the simplified model described above used for the parametric study.

A parametric study has been conducted to investigate the variation of directivity and S_{11} with cavity diameter, for types (A) and (B). Both inset and flush fed type (A) antennas showed a double peak in directivity as diameter was increased, Figure 3. The lower diameter directivity peak occurs between the diameters of $2.0\text{-}2.2\lambda_o$, with the inset feed having decreased the directivity by about 0.3dB. The good S_{11} and directivity of the inset fed $2.0\lambda_o$ diameter antenna explains its popularity with prior investigators. The inset feed however caused a $0.3\lambda_o$ difference in the diameter at which the higher directivity peak occurred and an approximately 0.6dB decrease in value, Figure 3. Addition of the curved juncture modified the directivity and S_{11} characteristics of both inset and flush fed cavities, Figure 3. Of interest is the $2.6\text{-}2.8\lambda_o$ diameter range in which the directivity of both inset and flush fed (B) designs peak, been at least 1dB higher than that of the type (A) antennas. The directivity peak of the inset (B) antenna was higher and was maintained across the broadest range of diameters suggesting a wider directivity bandwidth, although an input impedance matching network would be required for its use as an effective radiator.

Considering the inset fed designs, the highest aperture efficiency of the type (A) antenna occurred at a diameter of $2.4\lambda_o$ and at $2.6\lambda_o$ for the type (B) design, with directivities of 15.9dB and 17.4dB, respectively. Also, the type (B) antenna gave distinct nulls in the E-plane, unlike the type (A). So, the type (B) antenna has the advantages of higher directivity and nulls roughly in the direction of the expected grating lobes.

Comparing the inset fed $2.6\lambda_o$ diameter type (A) and (B) antennas, there was a directivity difference of 1.7dB, Figure 3. Inspection of the amplitude and phase in the principal planes $0.25\lambda_o$ above the aperture mouth shows that the differences are mostly in the E-plane, Figure 4. The range of E-plane aperture amplitude of the type (A) antenna was about 17dB, while it was 5.5dB for the type (B) design. The E-plane aperture phase of the type (A) design had a range of about 160°, while it was about 30° for type (B). Thus, addition of the curved juncture between the cavity base and rim has flattered both the aperture amplitude and phase distributions in the E-plane, resulting in a higher directivity.

Both the experimental and numerical results will be discussed in detail during the presentation. Consideration will also be given to waveguide inset depth, and stepped junctures which are more readily machined type (C), Figure 1.

5. Acknowledgements

Funding for this research was provided by TRLabs and the Canadian Institute for Telecommunications Research (CITR).

6. References

[1] T. Sehm, A. Lehto & A.V. Raisanen, "Large planar 39-GHz antenna array of waveguide fed horns", IEEE Trans. Antennas and Prop., v46 n8, Aug. 1998, pp 1186-1193.

[2] Y. Fujii, K. Yoshiki & T. Abiko, “Waveguide power feeding antenna”, Japanese patent H05-175,725A, July 13 1993.

[3] A.C. Large, "Short backfire antennas with waveguide and linear fields", Microwave Journal, v19 n8, Aug. 1976, pp 49-52.

[4] H. Koike, T. Abiko, Y. Fujii, H. Inoue & K. Tsukamoto, “Waveguide array antenna”, Japanese patent H02-223,206A, Sep 5 1990.

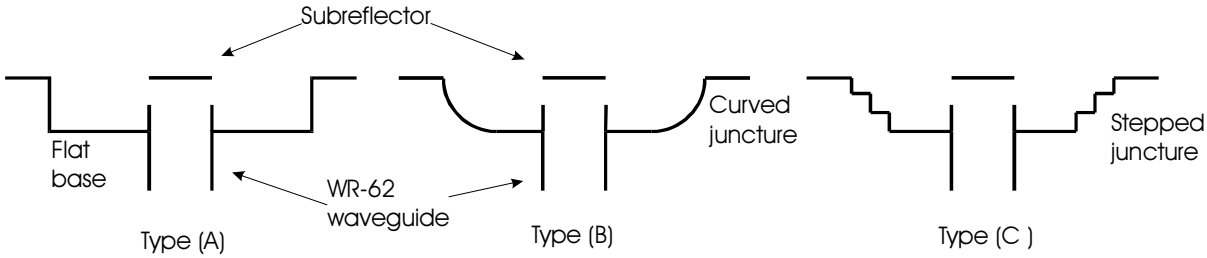

Figure 1: Circularly symmetric, inset fed SBA cavity profiles studied.

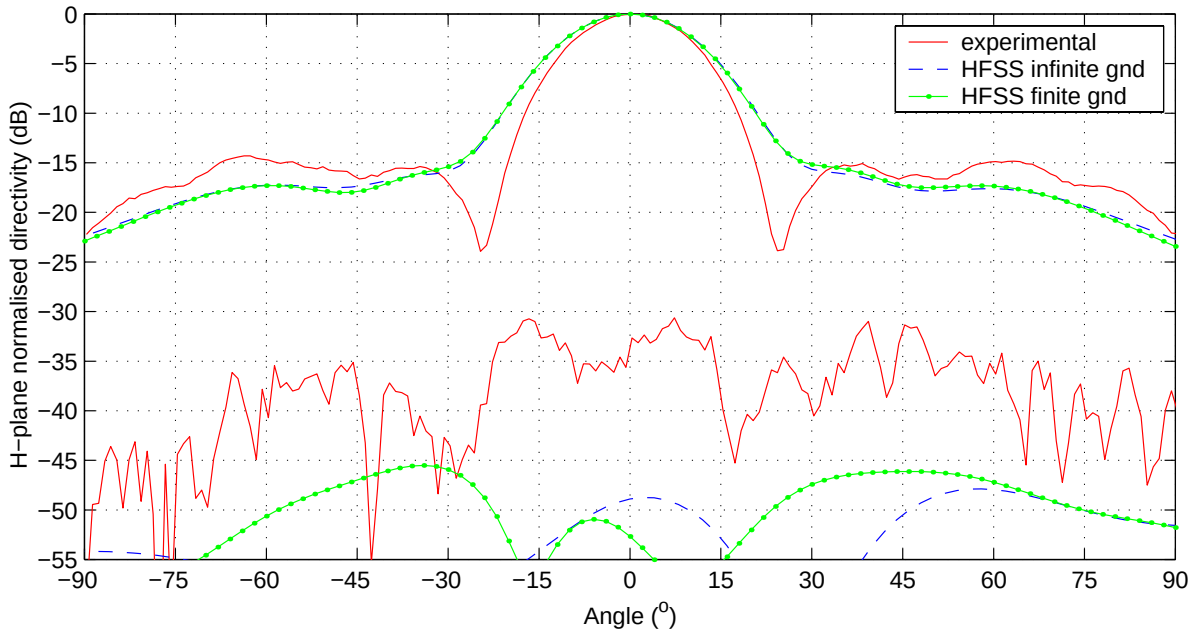

Figure 2: Comparison of experimental and HFSS H-plane radiation patterns of a $2.5\lambda_o$ diameter, inset fed, type (A) antenna, at 15GHz.

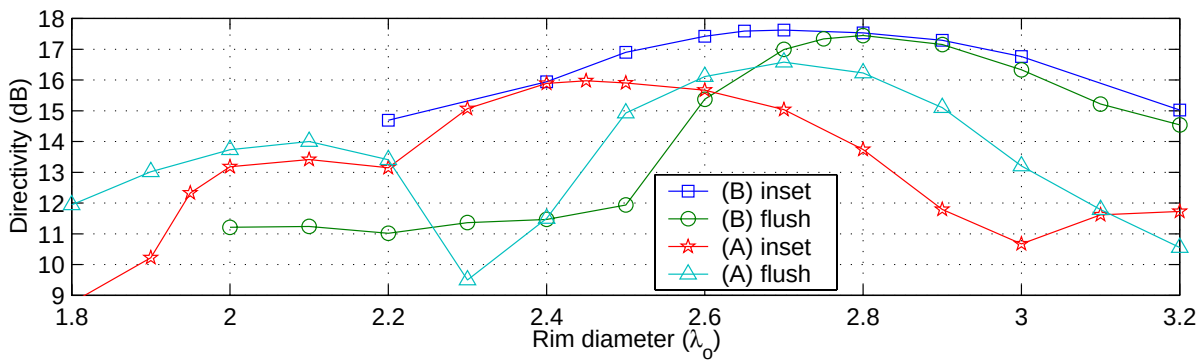

Figure 3: Directivity variation with increasing cavity diameter from HFSS, at 15GHz.

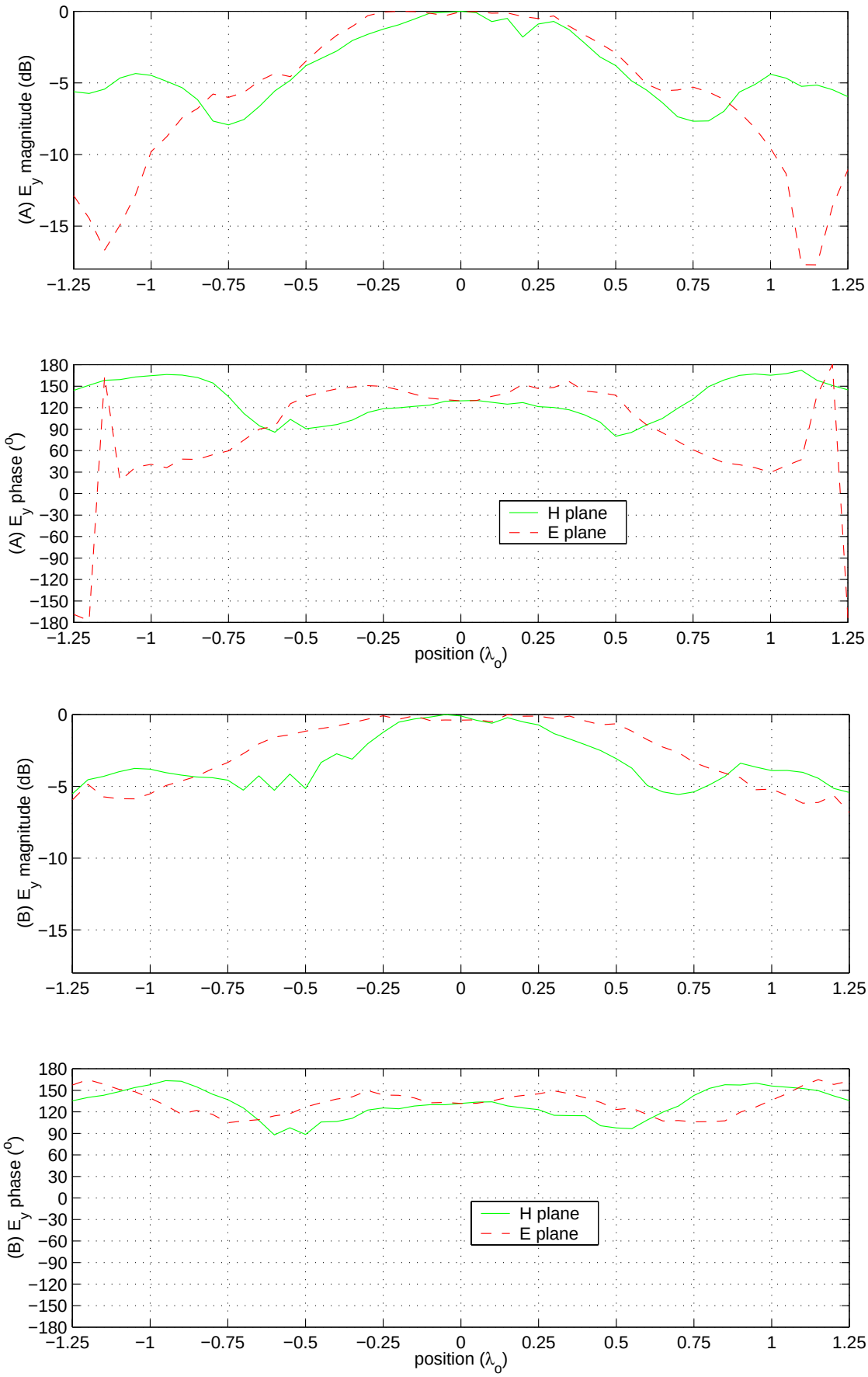

Figure 4: Comparison of aperture amplitude and phase distribution of inset fed 2.6λ_o diameter type (A) and type (B) antennas, from HFSS.